ChemPubSoc Europe
DOI: 10.1002/cmdc.201500382
CHEMMEDCHEM Full Papers

Aryl Bis-Sulfonamide Inhibitors of IspF from *Arabidopsis thaliana* and *Plasmodium falciparum*

Jonas Thelemann,[a] Boris Illarionov,[b] Konstantin Barylyuk,[a] Julie Geist,[a] Johannes Kirchmair,[c] Petra Schneider,[d] Lucile Anthore,[a] Katharina Root,[a] Nils Trapp,[a] Adelbert Bacher,[e] Matthias Witschel,*[f] Renato Zenobi,*[a] Markus Fischer,*[b] Gisbert Schneider,*[d] and François Diederich*[a]

2-Methylerythritol 2,4-cyclodiphosphate synthase (IspF) is an essential enzyme for the biosynthesis of isoprenoid precursors in plants and many human pathogens. The protein is an attractive target for the development of anti-infectives and herbicides. Using a photometric assay, a screen of 40000 compounds on IspF from *Arabidopsis thaliana* afforded symmetrical aryl bis-sulfonamides that inhibit IspF from *A. thaliana* (*At*IspF) and *Plasmodium falciparum* (*Pf*IspF) with IC_{50} values in the micromolar range. The *ortho*-bis-sulfonamide structural motif is essential for inhibitory activity. The best derivatives obtained by parallel synthesis showed IC_{50} values of 1.4 μm against *Pf*IspF and 240 nm against *At*IspF. Substantial herbicidal activity was observed at a dose of 2 kg ha^{-1}. Molecular modeling studies served as the basis for an in silico search targeted at the discovery of novel, non-symmetrical sulfonamide IspF inhibitors. The designed compounds were found to exhibit inhibitory activities in the double-digit micromolar IC_{50} range.

Introduction

Plants, many bacteria, and some protozoa, including numerous human pathogens, use the non-mevalonate pathway for the biosynthesis of isoprenoids.[1,2] This pathway is absent in humans and has been clinically validated as a druggable antimalarial target.[3,4] Following its discovery in the 1990s,[1,2,5] the pathway was shown to start with the condensation of pyruvate (**1**) and glyceraldehyde 3-phosphate (**2**) (Scheme 1). The consecutive action of six enzymes (IspC–IspH) performs the conversion into a mixture of isopentenyl diphosphate (IPP, **3**) and dimethylallyl diphosphate (DMAPP, **4**). The antepenultimate enzyme in this pathway, IspF, converts diphosphocytidyl-2-methylerythritol 2-phosphate (**5**) into 2-methylerythritol 2,4-cyclodiphosphate (**6**). This enzyme is active as a homotrimer, with the three active sites located between adjacent subunits.

Several IspF inhibitors have been reported, including substrate analogue ligands with dissociation constants (K_d) of 15 μm against IspF from *Escherichia coli*[6] and 70 μm against IspF of *Burkholderia pseudomallei* (*Bp*IspF).[7] We previously reported thiazolopyrimidine-derived *Pf*IspF inhibitors, discovered by high-throughput screening (HTS), with IC_{50} (median inhibitory concentration) values as low as 9.6 μm.[8]

Herein we report work on aryl bis-sulfonamides, a new class of IspF inhibitors, which were identified following the same HTS approach.[8] Derivatives **7**–**19** (Tables 1 and 2) of the original hit **7a** were synthesized, and their interaction with IspF was analyzed by biochemical, biophysical, and computational methods. The structure-based rational design and synthesis of novel aryl sulfonamide inhibitors **20a**–**g** (Table 3) is also reported.

Results and Discussion

Binding affinities of aryl bis-sulfonamide ligands

HTS on *At*IspF using a library of 40000 compounds afforded the *ortho*-bis-sulfonamide derivative **7a**. The compound (Table 1) was shown to inhibit *At*IspF and *Pf*IspF (see Section S5 in the Supporting Information for a schematic representation of the active sites of these enzymes) with respective IC_{50} values

[a] J. Thelemann, Dr. K. Barylyuk, Dr. J. Geist, L. Anthore, K. Root, Dr. N. Trapp, Prof. Dr. R. Zenobi, Prof. Dr. F. Diederich
Laboratorium für Organische Chemie, ETH Zürich
Vladimir-Prelog-Weg 3, 8093 Zürich (Switzerland)
Fax: (+41) 44-632-1109
E-mail: diederich@org.chem.ethz.ch
zenobi@org.chem.ethz.ch

[b] Dr. B. Illarionov, Prof. Dr. M. Fischer
Institut für Lebensmittelchemie, Universität Hamburg
Grindelallee 117, 20146 Hamburg (Germany)
E-mail: markus.fischer@chemie.uniso-hamburg.de

[c] Prof. Dr. J. Kirchmair
Zentrum für Bioinformatik, Universität Hamburg
Bundesstr. 43, 20146 Hamburg (Germany)

[d] Dr. P. Schneider, Prof. Dr. G. Schneider
Institut für Pharmazeutische Wissenschaften, ETH Zürich
Vladimir-Prelog-Weg 4, 8093 Zurich (Switzerland)
E-mail: gisbert.schneider@pharma.ethz.ch

[e] Prof. Dr. A. Bacher
Lehrstuhl für Biochemie, Technische Universität München
Lichtenbergerstr. 4, 85748 Garching (Germany)

[f] Dr. M. Witschel
BASF SE, Carl-Bosch-Str. 38, 67056 Ludwigshafen (Germany)
E-mail: matthias.witschel@basf.com

Supporting information for this article is available on the WWW under http://dx.doi.org/10.1002/cmdc.201500382.

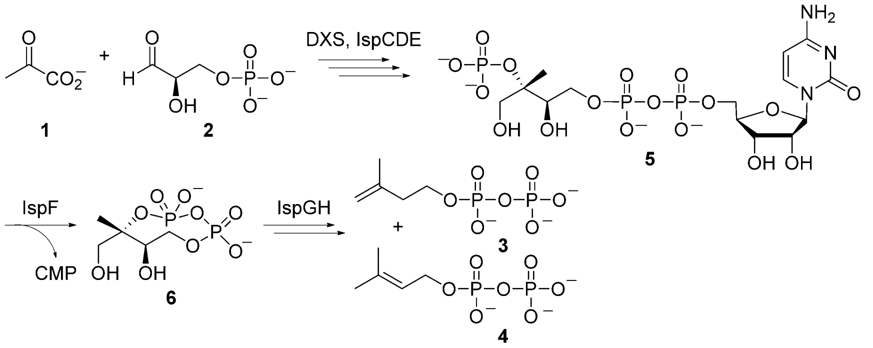

Scheme 1. Non-mevalonate pathway of isoprenoid biosynthesis focusing on the transformation catalyzed by IspF.

Table 1. Inhibition of recombinant *A. thaliana*, *P. falciparum*, and *B. pseudomallei* IspF by symmetric aryl bis-sulfonamides.

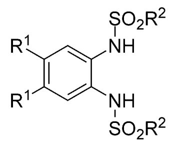

Compd	R^1	R^2	IC_{50} [μM][a] *At*IspF	*Pf*IspF	*Bp*IspF	clog*P*[b]	clog*D*[c]
7a	NO_2	*p*-tolyl	18±4	1.9±0.4	173±11	3.9	4.4
7b	NO_2	*c*Pr	35±15	7.7±1.8	>500	0.9	0.2
7c	NO_2	*n*Hex	–[d]	–[d]	54±23	4.3	4.7
7d	NO_2	CH_2CF_3	17±5	21±4	226±16	2.0	3.0
7e	NO_2	Ph	13±5	2.7±0.5	296±25	3.2	3.5
7f	NO_2	4-Br-C_6H_4	0.69±0.3	1.4±0.2	101±17	4.6	5.5
7g	NO_2	4-OMe-C_6H_4	7.7±2	4.8±0.9	311±22	2.7	4.5
7h	NO_2	4-O(*n*Bu)C_6H_4	12±2	1.4±0.2	44±7	4.6	7.7
7i	NO_2	4-CF_3-C_6H_4	4.6±1	4.6±1	123±13	4.2	5.4
8a	Br	*p*-tolyl	5.6±0.5	13±1	70±3	5.7	6.5
8b	Br	4-Br-C_6H_4	0.53±0.3	1.4±0.5	23±7	6.1	6.7
8c	Br	3-Br-C_6H_4	0.25±0.05	3.8±0.8	–[e]	6.4	7.1
8d	Br	2-Br-C_6H_4	0.74±0.15	8.3±0.08	–[e]	6.3	5.8
8e	Br	4-O(*n*Bu)C_6H_4	1.5±1.2	2.1±1.1	61±16	6.3	9.4
8f	Br	4-CF_3-C_6H_4	1.8±0.2	1.4±0.4	21±16	6.4	6.5
8g	Br	4-OCF_3-C_6H_4	0.47±0.1	5.6±0.7	–[e]	5.7	7.6
8h	Br	3,5-bis(CF_3)C_6H_4	0.3±0.07	4.0±0.9	–[e]	7.3	8.4
8i	Br	2-thiophenyl	53±15	22±3	–[e]	4.5	3.7
8j	Br	4-Br-$CH_2C_6H_4$	0.24±0.04	5.5±0.5	–[e]	6.4	6.7
8k	Br	3-pyridyl	>500	30±3	–[e]	3.0	2.1
9a	H	*p*-tolyl	40±12	29±9	>500	3.2	4
9b	H	*c*Pr	>500	281±24	>500	1.2	0.7
9c	H	*n*Hex	–[d]	–[d]	>500	4.4	5.2
9d	H	CH_2CF_3	77±21	52±10	>500	2.1	1.6
9e	H	2-thiophenyl	>500	181±50	–[e]	2.9	0.9
10	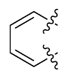	*p*-tolyl	1.4±0.4	62±10	–[e]	5.7	5.9
11	Me	*p*-tolyl	>500	>500	–[e]	5.1	5.9
12	CN	*p*-tolyl	48±12	7.8±2	–[e]	3.7	3.2
13	Ph	*p*-tolyl	50±11	22±4	–[e]	6.1	7.6

[a] Assay buffer: 100 mM Tris·HCl (pH 8.0); error margins correspond to the RMSD of the regression fit (Section S2 in the Supporting Information for details). [b] Values were calculated with the ACD/Percepta[43] software package (GALAS algorithm). [c] Values were calculated with ACD/Percepta[43] at pH 8.0. [d] Data were not interpretable. [e] Inhibition was not determined. Inhibition by compounds **9f**–**p** was not determined.

of 18 and 1.9 μM, based on initial rate measurements at a substrate concentration of 0.5 mM. In an attempt to improve these values, a series of symmetric *ortho*-bis-sulfonamide derivatives **7**–**13** was synthesized (Scheme 2). Diamines **21a**–**c** were treated with the corresponding sulfonyl chlorides to yield compounds **9**–**11**. R^1 groups were subsequently introduced by nitration of **9** to yield compounds **7a**–**i**, or bromination to afford compounds **8a**–**k**. Compound **12** was formed by cyanation of aryl bromide **8a**,[9] whereas Suzuki cross-coupling of **8a** with phenylboronic acid yielded inhibitor **13**.

All synthesized compounds **7**–**13** were tested using the previously reported photometric assay[10] with IspF isoforms from *A. thaliana*, *P. falciparum*, and *B. pseudomallei* (Table 1). Typical inhibition curves are shown in Section S2 of the Supporting Information. Notably, **8f** inhibits *Pf*IspF with an IC_{50} value of 1.4 μM, and **8j** inhibits *At*IspF with an IC_{50} value of 0.240 μM.

Our photometric assay couples the enzyme activity of IspF with the oxidation of NADH via a cascade of auxiliary enzymes to enable photometric detection.[10] Most of the studied compounds were verified to not inhibit these auxiliary enzymes (Section S3, Supporting Information). To rule out any contamination of the results via inhibition of auxiliary enzymes, we used an HPLC-based assay to directly determine the IspF-mediated conversion of **5** into **6**, without any auxiliary components.[11] However, we emphasize that the HPLC assay is an end-point assay, with samples analyzed after a predetermined incubation period, whereas the multicomponent assay measures initial rates. The HPLC assay was applied to the most promising inhibitor/orthologue combinations, with appar-

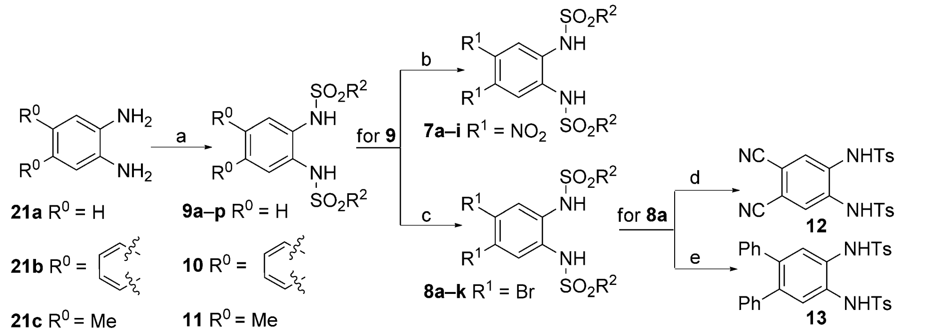

Scheme 2. Synthesis of compounds **7**–**13**. A list of R^2 substituents is provided in Table 1. *Reagents and conditions*: a) R^2SO_2Cl, CH_2Cl_2, pyridine, 25 °C, 12 h; b) HNO_3, AcOH, 60 °C, 30 min; c) Br_2, NaOAc, AcOH, 25–100 °C, 1 h; d) CuCN, DMF, 120 °C, 20 h; e) phenylboronic acid, Cs_2CO_3, [Pd(dppf)Cl_2]·CH_2Cl_2, 1,4-dioxane, 90 °C, 2 h. Ts = *p*-toluenesulfonyl; dppf = 1,1′-bis(diphenylphosphino)ferrocene.

ent IC_{50} values in the nanomolar or low single-digit micromolar range, according to the multicomponent assay. As shown in Section S4 in the Supporting Information, the apparent IC_{50} values determined by the two different assay methods were found to be in agreement, within narrow margins.

The results listed in Table 1 show that nitro or bromo substituents at the R^1 positions of the ligands were conducive to strong inhibitory activity. Compounds **7a** ($R^1 = NO_2$) and **8a** (R^1 = Br) show IC_{50} values of 1.9 and 13.1 μM against *Pf*IspF, whereas **9a** (R^1 = H) has an IC_{50} value of 29 μM and compound **11** (R^1 = Me) is inactive ($IC_{50} > 500$ μM). These findings correlate with the measured pKa_1 values (Section S7, Supporting Information) for the first sulfonamide NH deprotonation, which is lower for compounds **7a** (pK_{a1} = 3.7) and **8a** (pK_{a1} = 5.9) than for **9a** (pK_{a1} = 7.9) and **11** (pK_{a1} = 7.5), suggesting that the bis-sulfonamides bind in a deprotonated state to the enzyme, as the activity assays were performed at pH 8.0.

Compound **8b** was also assayed for herbicidal activity in the greenhouse (Section S6, Supporting Information) and showed very good activity (+++) against *Setaria viridis*, *Echinochloa crusgalli*, and *Apera spica-venti* at a dose of 2 kg ha^{-1}. Ligands **7**–**9** were tested for antimalarial activity using a [^{3}H]hypoxanthine incorporation assay,[12] but failed to inhibit the proliferation of blood-stage *P. falciparum* (EC_{50} values > 5 mM).

To determine whether the molecular symmetry of *ortho*-bis-sulfonamides is essential for IspF inhibition, we prepared the non-symmetric derivatives **14**–**16** (Scheme 3). Moreover, several monosulfonamides **17**–**19** were synthesized. Specifically, compound **21d** was treated with chlorosulfonic acid followed by ammonia to provide sulfonamide **22**, which was reacted with 4-bromobenzenesulfonylchloride to give **14**. Amines **21a**, **21e**, **21f**, and **21g** were reacted with the corresponding arylsulfonyl chloride to give **23**–**26** and **19**, respectively. Bromination provided compounds **15**–**18**.

The non-symmetric bis-sulfonamides **14**–**16** exhibited weak activity, and the monosulfonamides **17**–**19** little or no inhibitory activity (Table 2). Similar to the other sulfonamide ligands reported herein, the solubility of the compounds is high, enabling all the physical studies performed.

Bis-sulfonamides are known to chelate metal cations.[13,14] We recorded the crystal structures of free ligand **8a** and of its dianion forming a 2:1 host–guest complex with Zn^{2+} (Figure 1). The two sulfonamide moieties of free **8a** have torsional angles of N(2)-S(2)-C(8)-C(9) = 104° and N(1)-S(1)-C(5)-C(14) = 101°, which is close to the preferred N-S-C-C torsional angle of 90°. As observed before, the nitrogen lone pair bisects the O-S-O fragment.[15] The four N-S-C-C torsional angles for the complex of

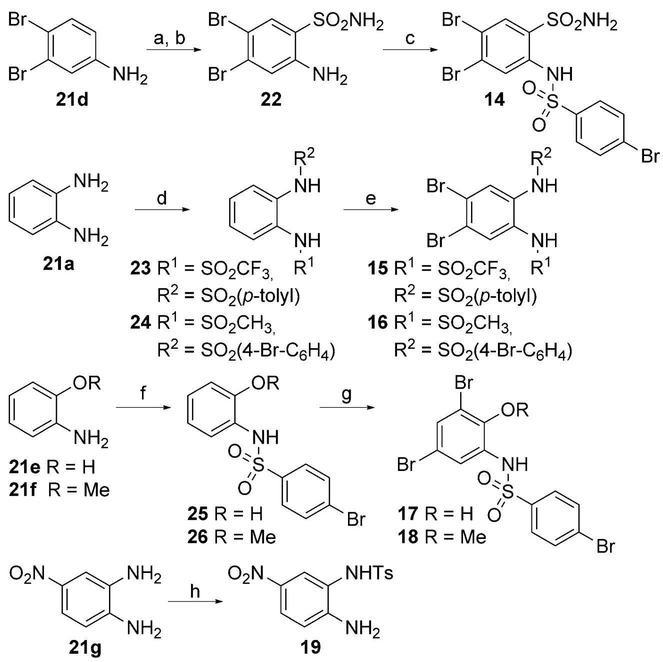

Scheme 3. Synthesis of non-symmetric sulfonamides **14**–**19**. *Reagents and conditions*: a) SO_2Cl_2, 150 °C, 3 h; b) NH_3, 1,4-dioxane, 25 °C, 30 min; c) 4-bromobenzenesulfonyl chloride, CH_2Cl_2, pyridine, 25 °C, 12 h; d) R^1SO_2Cl, R^2SO_2Cl, CH_2Cl_2, pyridine −78–25 °C, 12 h; e) Br_2, NaOAc, AcOH, 25–100 °C, 1 h; f) 4-bromobenzenesulfonyl chloride, CH_2Cl_2, pyridine, 25 °C; g) Br_2, NaOAc, AcOH, 25–100 °C, 1 h; h) 4-toluenesulfonyl chloride, CH_2Cl_2, pyridine 25 °C, 12 h.

8a with Zn^{2+} are identical at 38°. The Zn^{2+} ion is tetrahedrally coordinated, with the four Zn···N distances being 2.00 Å.

Isothermal titration calorimetry (ITC) experiments at 303 K in Tris hydrochloride buffer (0.1 M)/$(CH_3)_2SO$ 2:1 confirmed that bis-sulfonamides **8a** and **8b** bind to the Zn^{2+} ion with apparent association constants (K_{app}) of 7.7×10^6 and 15.6×10^6 M^{-2} Therefore, it appeared possible that depletion of the essential Zn^{2+} cofactor in IspF could cause the observed inhibitory action of the studied compounds. However, compounds **7a**, **7f**, **7g**, **8a**, **8b**, and **8f** caused undiminished IspF inhibition in

Table 2. Inhibition of recombinant *A. thaliana* and *P. falciparum* IspF by the non-symmetric sulfonamides **14**–**19**.

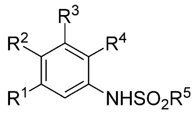

Compd	R1	R2	R3	R4	R5	IC_{50} [µM][a] *At*IspF	*Pf*IspF	clog*P*[b]	clog*D*[c]
14	Br	Br	H	SO_2NH_2	4-Br-C_6H_4	301±46	42±4	3.9	3.8
15	Br	Br	H	$NHSO_2CF_3$	*p*-tolyl	23±5	14±2	5.6	4.7
16	Br	Br	H	$NHSO_2CH_3$	4-Br-C_6H_4	>500	56±6	3.9	3.1
17	Br	H	Br	OH	4-Br-C_6H_4	133±5	>500	4.6	4.1
18	Br	H	Br	OMe	4-Br-C_6H_4	>500	>500	5.4	4.4
19	NO_2	H	H	NH_2	*p*-tolyl	272±25	177±30	2.0	3.0

[a] Assay buffer: 100 mM Tris·HCl (pH 8.0); error margins correspond to the RMSD of the regression fit (Section S2 in the Supporting Information for details). [b] Values were calculated with the ACD/Percepta[43] software package (GALAS algorithm). [c] Values were calculated with ACD/Percepta[43] at pH 8.0.

HEPES, 150 mM NaCl, pH 8.0; $T=298$ K) revealed a K_d value of 17 µM with fitting parameters $\Delta H^o = -5.9\ \mathrm{kJ\,mol^{-1}}$, $T\Delta S^o = 21.3\ \mathrm{kJ\,mol^{-1}}$, and $\Delta G^o = -27.2\ \mathrm{kJ\,mol^{-1}}$. Complexation is strongly entropically and weakly enthalpically driven. The substantial increase in entropy hints at the desolvation of ionic residues in both ligand and enzyme upon coordination.[16–18] The stoichiometric factor *n* was determined at 2.3 (IspF monomer: **8b**), which leads to a stoichiometry of 1.3 ligands per IspF trimer.

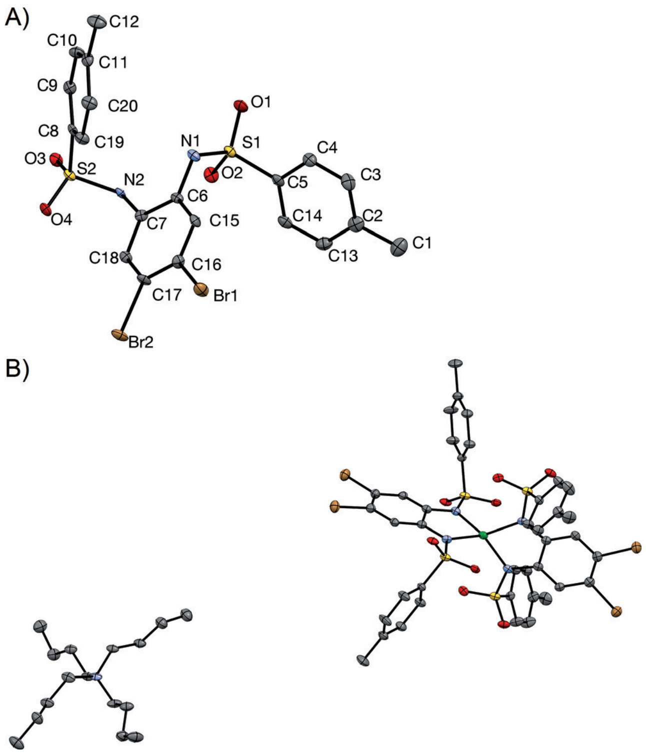

Figure 1. A) ORTEP plot at the 50% probability level of the crystal structure of inhibitor **8a**. B) ORTEP plot at the 15% probability level of the crystal structure of the 2:1 complex of dianionic ligand **8a** with Zn^{2+}. One of the two NBu_4^+ counterions is shown. $T=100$ K, arbitrary numbering. See Section S13 in the Supporting Information for further information.

the photometric assay in the presence of $Zn(OAc)_2$ (ligand/$Zn(OAc)_2$=2:1, see Table 1SI, Supporting Information). Hence, the observed inhibition of IspF by bis-sulfonamide compounds is not a consequence of Zn^{2+} depletion of the enzyme by the inhibitors.

Isothermal titration calorimetry (Section S12, Supporting Information) using **8b** and *At*IspF in ITC buffer (50 mM

ESI-MS binding studies

The binding affinity of **8b** for *At*IspF was also studied by direct titration in native ESI-MS (Section S10, Supporting Information). This method allows evaluation of protein–ligand affinities, binding stoichiometry, and allosteric effects.[19,20] Advantageously, measurements can be conducted with low ligand and enzyme concentrations.

Enzymes are believed to largely retain their folded, solution-like conformation in the gas phase when ionized by ESI under gentle desolvation and ion-transfer conditions, often referred to as "native ESI-MS".[21] Proteins and protein complexes can be detected as distinct signals to allow direct readout of the complex composition and stoichiometry. Moreover, in the case of enzyme–inhibitor binding, relative intensities of the free and ligand-bound enzyme peaks in mass spectra can be treated as the relative abundances of the respective species in solution. This gives direct access to solution-phase binding affinity determination by native ESI-MS.[22–24] The binding affinity of **8b** was measured at different ligand concentrations ranging from 1.6 to 50 µM with an enzyme concentration of 4.7 µM (Figure 2). The observed peak broadening can be attributed to residual solvent molecules and buffer ions that remain bound to the protein under the gentle desolvation conditions used. The peak at 54964 Da (calculated protein mass: 54984 Da) represents the *At*IspF trimer without a bound ligand. The peaks at 55668, 56372, and 57076 Da represent protein molecules bound to one, two, or three inhibitor molecules, respectively. No more than three ligands per trimer were observed. As the ligand concentration increases, the peak intensities of the enzyme–inhibitor complexes increase. The dissociation constant K_d was determined by applying the Hill equation[25] to the data on the fraction of bound ligand concentration determined from the mass spectra (Figure 2). We obtained K_d= 21 µM and a Hill parameter value $n_H=1.5$. The mass spectrometric dissociation constant and the value obtained by ITC (K_d=17 µM) are in remarkably good agreement, but higher than the calculated K_i value of 0.26 µM using the Cheng–Prus-

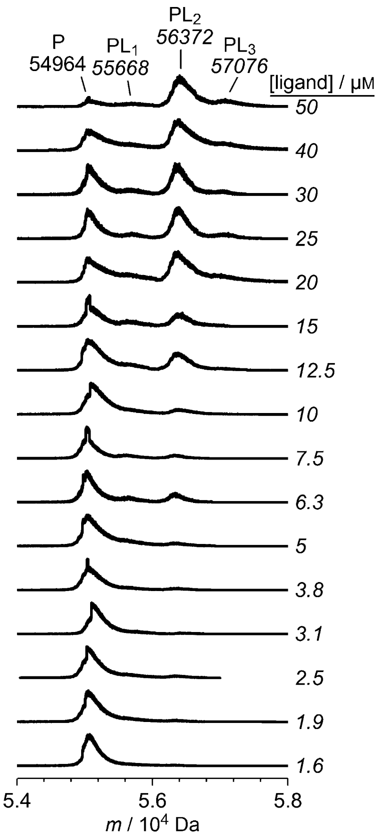

Figure 2. ESI-MS spectra of *At*IspF (at 4.7 μM) titrated with ligand **8b**. The spectral region of the protein trimer is displayed, and the various concentrations of **8b** are indicated next to the traces.

off equation on the inhibitory data from the photometric assay.[26,27]

Docking studies

Attempts to obtain a co-crystal structure of an aryl bis-sulfonamide inhibitor bound to IspF were unsuccessful. We used automated ligand docking in an attempt to investigate the binding mode of **8b** (Figure 3). The co-crystal structures of *A. thaliana* with CDP (PDB ID: 2PMP[28]) and *P. falciparum* with CMP as ligand (PDB ID: 4C81[29]) served as templates for the in silico studies. In light of the ligand's first pK_a value of 5.9, one of the sulfonamide nitrogen atoms of the symmetric molecule was assumed to be deprotonated. GOLD[30,31] was used for docking, ChemPLP[32] for scoring, and MOLOC[33] for geometric optimization of the docking poses. Further details are provided in Section S8 in the Supporting Information.

Due to steric hindrance, the anionic nitrogen of **8b** is unable to coordinate to the essential Zn^{2+} ion of IspF. However, the docking suggests that **8b** could form a salt bridge with its deprotonated sulfonamide motif to Lys135 (Lys213 for *P. falciparum*) at the active site. Furthermore, the second sulfonamide moiety can bind with its SO_2 group to the Zn^{2+} ion. It is known from enzymes containing catalytic Zn^{2+} ions that the primary coordination sphere of the metal can be trigonal bipyrimidal or square pyramidal (T5, 44% of all cases[34]). Thus, the T5 coordination to the catalytic zinc ion of *At*IspF, predicted by GOLD, is possible. It was recently well established that binding to the Zn^{2+} ion of IspF from different species under replacement of the fourth (water) ligand only yields a weakly enhanced binding affinity;[7,35] in other words, the SO_2 group as weakly binding ligand is a good possibility.

Monosulfonamide inhibitors derived by rational design

Despite the reported poor gain in binding affinity upon substituting the fourth water coordination site to the Zn^{2+} ligand by other donor ligands,[7,35] we wanted to probe this once more with inhibitors that feature a sterically unencumbered primary sulfonamide as zinc binding group linked to a cytosine derivative that docks into Pocket III of the active site.

Compounds **20a–g** (Scheme 4) were derived by molecular modeling using MOLOC.[33] Compound **20a** (Figure 4) was designed to bind with its 3-aminoisoquinoline ring (similar to ligands containing a 2-aminopyridine moiety for occupancy of the same pocket)[36] to the cytosine binding Pocket III. The heterocyclic nitrogen atom was predicted to interact with the

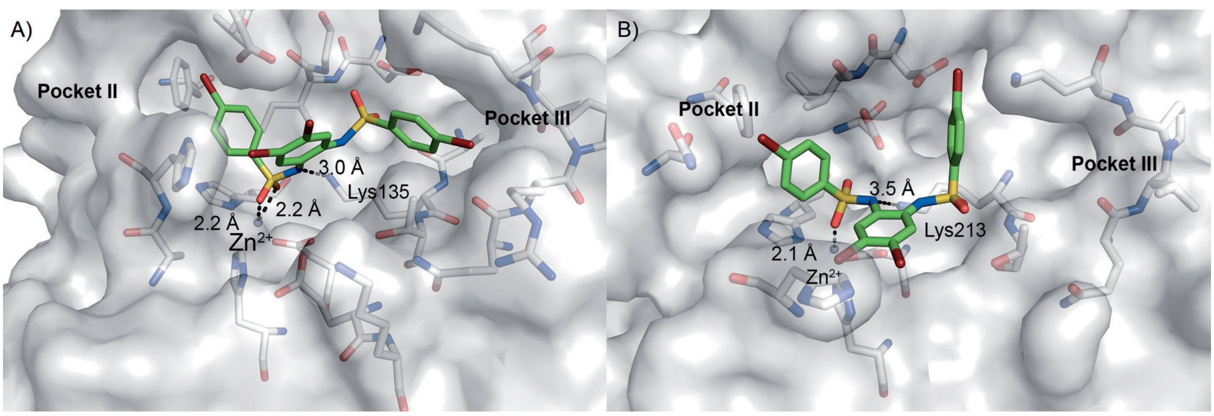

Figure 3. Ligand binding poses predicted for **8b** using GOLD for docking, ChemPLP for scoring, and MOLOC for optimization. A) *At*IspF; B) *Pf*IspF. The docking poses represent the highest-ranked solutions (ChemPLP scores: 73.62 and 71.77, respectively). Color code: C_{enzyme} gray, O red, N blue, S yellow, Br dark red, C_{ligand} green.

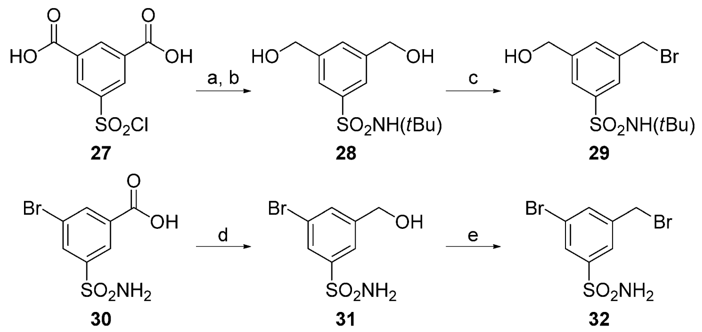

Scheme 4. Synthesis of building blocks **29** and **32**. *Reagents and conditions*: a) tBuNH$_2$, CH_2Cl_2, 0→23 °C, 1 h; b) BH_3, THF, 0→23 °C, 15 h; c) NBS, PPh_3, THF, 0→25 °C, 30 min; d) BH_3, THF, 0→23 °C, 1 h; e) PBr_3, CH_2Cl_2, 23 °C, 24 h. NBS = *N*-bromosuccinimide; THF = tetrahydrofuran.

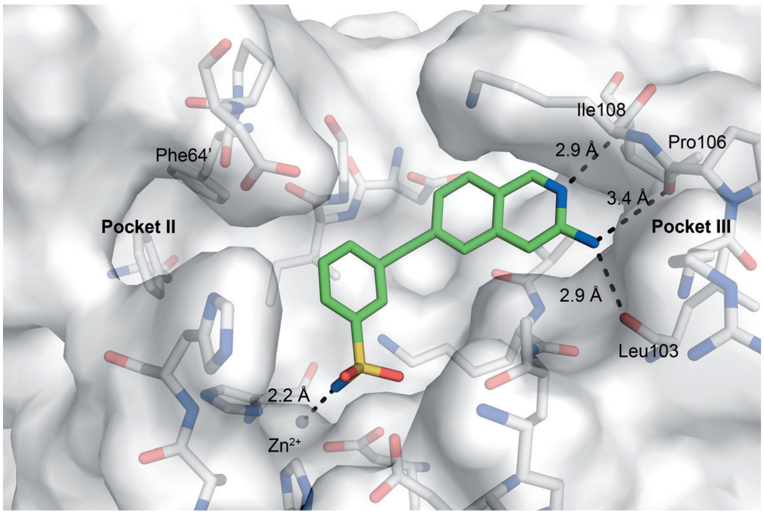

Figure 4. Proposed binding mode of **20a** in the active site of *At*IspF (PDB ID: 2PMP), modeled with MOLOC. Color code: C_{enzyme} gray, O red, N blue, S yellow, C_{ligand} green.

backbone NH of Ile108, (d(N···NH$_{Ile108}$) = 2.9 Å), whereas the exocyclic NH_2 group should undergo hydrogen bonding to the backbone C=O groups of Pro106 (d(NH$_2$···O=C$_{Pro106}$) = 3.4 Å) and Leu103 (d(NH$_2$···O=C$_{Leu103}$) = 2.9 Å). Similar to the binding of inhibitors with a primary sulfonamide to carbonic anhydrase,[37] the Zn^{2+} ion should coordinate to the deprotonated primary sulfonamide nitrogen atom (Figure 4).

The moderate activity of compound **20a**, with IC_{50} values of 561 ± 92 μм against *At*IspF and 287 ± 42 μм against *Pf*IspF, led us to design compounds **20b–g**, which feature additional substituents *meta* to the sulfonamide group to provide binding to the flexible hydrophobic Pocket II (Table 3). Compounds **20b–e** were designed to undergo hydrogen bonding to the backbone C=O of Phe64 (Figure 4), whereas compounds **20f** and **20g** exhibit a hydrophobic group to interact with the hydrophobic Pocket II.

Synthesis and biological activity of designed monosulfonamide ligands

5-(Chlorosulfonyl)isophthalic acid (**27**) was converted into compound **28**, then monobrominated to provide building block **29** (Scheme 4). Precursor **30** was prepared following a published protocol,[38] reduced to alcohol **31**, and brominated to afford building block **32**.

3-Aminoisoquinoline precursor **33** was synthesized according to published procedures[39,40] and Boc protected to afford compound **34**. One-pot borylation, followed by coupling to 3-bromobenzenesulfonamide and deprotection, afforded **20a** (Scheme 5). Borylation of compound **34**, coupling to building block **29** (Scheme 4), and oxidation provided aldehyde **35**, whereas borylation of compound **34** and coupling to building block **32** (Scheme 4) gave aryl bromide **36**. Bromides at benzylic positions react faster than aryl bromides;[41] therefore, the selective coupling of compounds **32** and **34** could be achieved.

Reductive amination of aldehyde **35** with the corresponding amines afforded inhibitors **20b–d**. Suzuki cross-coupling of compound **36** with the corresponding boronic ester/acid provided, after deprotection, compounds **20e–g**.

Compounds **20b–d**, which had been expected to form a hydrogen bond with the backbone C=O of Phe64 in the hydrophobic Pocket II, showed little to no biological activity (Table 3). More success was achieved with those inhibitors that feature hydrophobic substituents to fill the flexible Pocket II (see Section S5 in the Supporting Information for an overlay of various X-ray structures showing the large conformational flexibility of this pocket). The most active *Pf*IspF inhibitors developed by rational design were compounds **20f** (R = phenyl) and **20g** (R = 4-CF_3-C_6H_4), with IC_{50} values of 39 and 45 μм, respectively.

Conclusions

We presented aryl bis-sulfonamides as a new class of IspF inhibitors, identified by HTS. They are the most active IspF inhibitors reported so far, with IC_{50} values as low as 240 nм against *At*IspF and 1.4 μм against *Pf*IspF. The inhibition was measured by an enzyme-coupled photometric assay and was confirmed for the most active inhibitors by an alternative HPLC assay. The binding affinities (K_d values) were determined by ITC and ESI-MS to be 17 μм and 21 μм, respectively. The binding mode of

Table 3. Inhibition of recombinant *A. thaliana*, *P. falciparum*, and *M. tuberculosis* IspF by ligands **20 a–g**.

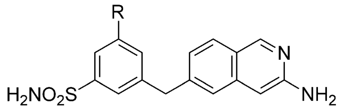

Compd	R	IC_{50} [μM][a]			clogP[b]	clogD[c]
		*At*IspF	*Pf*IspF	*Mt*IspF		
20 a	H	561 ± 92	287 ± 42	–[d]	2.2	1.9
20 b	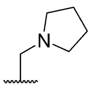	> 1000	> 1000	–[d]	2.5	0.3
20 c	CH_2NHEt	> 1000	939 ± 290	–[d]	2.6	0.3
20 d	CH_2NH*c*Pr	846 ± 113	632 ± 142	–[d]	2.6	1.2
20 e	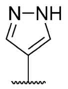	296 ± 946	170 ± 20	–[d]	2.3	1.9
20 f	Ph	> 1000	39 ± 23	59 ± 3	3.6	3.7
20 g	4-CF_3-C_6H_4	76 ± 15	45 ± 6	43 ± 19	5.0	4.7

[a] Error margins correspond to the RMSD of the regression fit (see Section S2 in the Supporting Information). [b] Values were calculated with the ACD/Percepta[43] software package (GALAS algorithm). [c] Values were calculated with ACD/Percepta[43] at pH 8.0. [d] Values not determined.

bis-sulfonamide ligand **8 b** was investigated by using a docking approach. In the proposed most favorable geometry, the deprotonated sulfonamide of the ligand undergoes ion pairing with the side chain of Lys135 and does not bind to the Zn^{2+} ion at the active site of IspF. However, the metal ion interacts with the SO_2 group of the second sulfonamide moiety in the ligand.

Using a molecular modeling approach, we further developed a series of inhibitors with a 3-aminoisoquinoline moiety to bind to the cytosine Pocket III, a terminal sulfonamide moiety to coordinate to the Zn^{2+} ion, and a vector addressing the region of the flexible Pocket II. Whereas attempted hydrogen bonding to the C=O group of Phe64 at the entrance of Pocket II was unsuccessful, significant binding affinity could be gained by filling the flexible hydrophobic parts of this pocket, with measured IC_{50} values down to 39 μM.

Experimental Section

Biology

Recombinant IspF proteins from *A. thaliana*, *P. falciparum*, *M. tuberculosis* and *B. pseudomallei*, and cytidylate kinase from *E. coli* were prepared as reported elsewhere.[8,10] Adenylate kinase and lactate dehydrogenase were purchased from Sigma–Aldrich. NADH was purchased from Acros Organics. See the Supporting Information for a description of the biological assays and pK_a measurements.

Chemistry

Materials: Experimental details for the synthesis of ligand **20 g** are reported below. The synthesis of all other compounds, ESI-MS and ITC measurements, and details of the molecular docking studies are provided in the Supporting Information. Structural models of the protein were visualized in PyMOL.[42]

***N*,*N*-Bis(*tert*-butoxycarbonyl)-6-bromoisoquinolin-3-amine (34)**: A solution of isoquinoline **33** (553 mg, 2.48 mmol) and 4-(dimethylamino)pyridine (31 mg, 0.26 mmol) in CH_3CN was cooled to 0 °C, treated with di-*tert*-butyl dicarbonate (1.67 g, 7.67 mmol) and NEt_3 (1.70 mL, 12.3 mmol), and stirred for 2 h at 0 °C and then for 20 h at 23 °C. Evaporation and chromatography (SiO_2, cyclohexane/

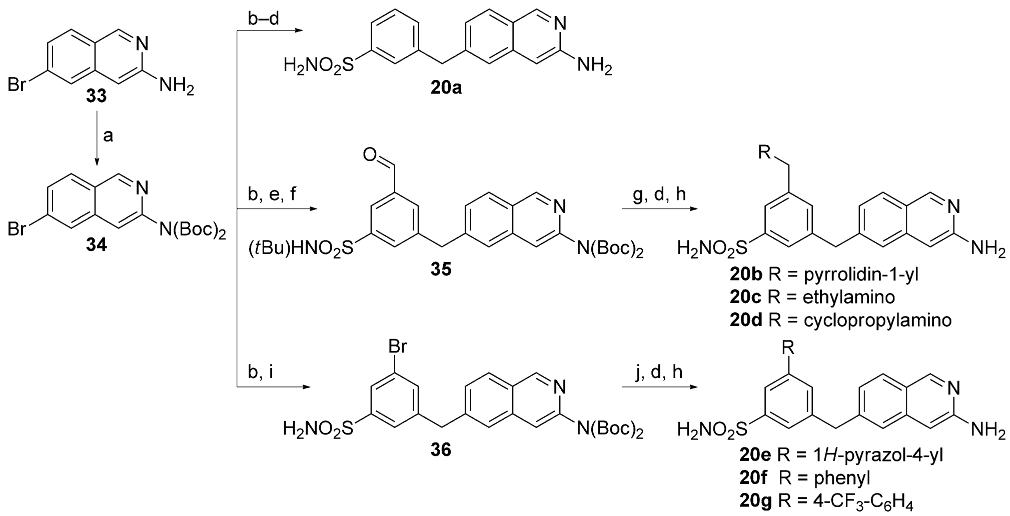

Scheme 5. Synthesis of **20 a–g**. *Reagents and conditions*: a) Boc_2O, DMAP, NEt_3, CH_3CN, 0–24 °C, 24 h; b) $(BPin)_2$, KOAc, $[Pd(dppf)Cl_2]\cdot CH_2Cl_2$, 1,4-dioxane, 80 °C, 4 h; c) 3-(bromomethyl)benzenesulfonamide, Cs_2CO_3, $[Pd(dppf)Cl_2]\cdot CH_2Cl_2$, 1,4-dioxane/$H_2O$ (10:1), 80 °C, 12 h; d) CF_3COOH, CH_2Cl_2, 25 °C, 12 h; e) **29**, Cs_2CO_3, $[Pd(dppf)Cl_2]\cdot CH_2Cl_2$, 1,4-dioxane/$H_2O$ (10:1), 80 °C, 2 h; f) DMP, CH_2Cl_2, 25 °C, 5 h; g) RH, $NaBH(OAc)_3$, CH_2Cl_2, 25 °C, 80 min; h) CF_3COOH, 70 °C, 90 min; i) **32**, Cs_2CO_3, $[Pd(dppf)Cl_2]\cdot CH_2Cl_2$, 1,4-dioxane/$H_2O$ (10:1), 80 °C, 2 h; j) $RB(OH)_2$, Cs_2CO_3, $[Pd(dppf)Cl_2]\cdot CH_2Cl_2$, 1,4-dioxane/$H_2O$ (10:1), 80 °C, 50 min. Boc = *t*-butoxycarbonyl; DMAP = 4-(dimethylamino)pyridine; Pin = pinacolato; DMP = Dess–Martin periodinane.

EtOAc 10:1→6:1) afforded **34** (426 mg, 41%) as a yellow resin. R_f = 0.46 (SiO_2, cyclohexane/EtOAc 2:1); mp: 82–85 °C; ^{1}H NMR (400 MHz, CD_3OD): δ = 1.40 (s, 18H, CH_3), 7.73 (br s, 1H, H-C(4)), 7.80 (dd, J = 8.8, 1.9 Hz, 1H, H-C(7)), 8.06 (d, J = 8.8 Hz, 1H, H-C(8)), 8.21 (d, J = 1.6 Hz, 1H, H-C(5)), 9.18 ppm (s, 1H, H-C(1)); ^{13}C NMR (101 MHz, CD_3OD): δ = 28.11, 84.56, 119.15, 127.22, 127.48, 130.03, 130.66, 132.65, 139.90, 148.60, 152.68, 152.89 ppm; IR (ATR): $\tilde{\nu}$ = 2979, 2933, 1789, 1752, 1717, 1620, 1367, 1355, 1306, 1272, 1243, 1150, 1111, 1059, 1025, 946, 901, 888, 851, 815, 775, 721 cm^{-1}; HR-ESI-MS: m/z (%): 425.0890 (10, $[M+H]^+$ calcd for $C_{19}H_{24}{}^{81}BrN_2O_4{}^+$: 425.0894), 423.0911 (12, $[M+H]^+$ calcd for $C_{19}H_{24}{}^{79}BrN_2O_4{}^+$: 423.0914), 325.0368 (37, $[M-CH_2{=}CMe_2-CO_2+H]^+$ calcd for $C_{14}H_{16}{}^{81}BrN_2O_2{}^+$: 325.0370), 323.0385 (34, $[M-CH_2{=}CMe_2-CO_2+H]^+$ calcd for $C_{14}H_{16}{}^{79}BrN_2O_2{}^+$: 323.0390), 268.9745 (91, $[M-2CH_2{=}CMe_2-CO_2+H]^+$ calcd for $C_{10}H_8{}^{81}BrN_2O_2{}^+$: 268.9744), 266.9764 (100, $[M-2CH_2{=}CMe_2-CO_2+H]^+$ calcd for $C_{10}H_8{}^{79}BrN_2O_2{}^+$ 266.9764).

3-Bromo-5-(hydroxymethyl)benzenesulfonamide (31): 3-Bromo-5-sulfamoylbenzoic acid (**30**, 2.30 g, 8.21 mmol) was dissolved in dry THF (10 mL), treated with a solution of 1 M BH_3 in THF (16.4 mL, 16.4 mmol), and stirred for 20 h at 23 °C. The mixture was cooled to 0 °C and treated with H_2O (15 mL). The aqueous layer was extracted with EtOAc (3×25 mL). The combined organic layers were dried over Na_2SO_4, filtered, concentrated, and washed with toluene (50 mL) to give **31** (2.16 g, 98%) as a white solid. R_f = 0.18 (SiO_2, CH_2Cl_2/MeOH 10:1); mp: 115–116 °C; ^{1}H NMR (400 MHz, CD_3OD): δ = 4.66 (s, 2H, CH_2), 7.74 (s, 1H, H-C(4)), 7.86 (s, 1H, H-C(6)), 7.93 ppm (s, 1H, H-C(2)); ^{13}C NMR (101 MHz, CD_3OD): δ = 63.67, 123.45, 123.86, 128.57, 133.88, 147.00, 147.03 ppm; IR(ATR): $\tilde{\nu}$ = 3663 (w), 3377 (s), (3263 (s), 3068 (m), 2988 (m), 2915 (m), 1760 (w), 1595 (m), 1568 (m), 1531 (m), 1456 (m), 1430 (m), 1403 (m), 1326 (very s), 1257 (m), 1208 (m), 1148 (very s), 1113 (s), 1104 (s), 1060 (s), 992 (m), 916 (s), 885 (m), 873 (s), 857 (s), 780 (m), 695 (w), 671 (s), 631 cm^{-1} (m); HR-ESI-MS (negative mode): m/z (%): 265.9313 (100, $[M-H]^-$ calcd for $C_7H_7{}^{81}BrNO_3S^-$: 265.9314), 263.9334 (100, $[M-H]^-$ calcd for $C_7H_7{}^{79}BrNO_3S^-$: 263.9335).

3-Bromo-5-(bromomethyl)benzenesulfonamide (32): A suspension of sulfonamide **31** (1.40 g, 5.26 mmol) in CH_2Cl_2 (50 mL) was treated with PBr_3 (600 µL, 6.31 mmol) at 23 °C, stirred for 24 h, diluted with H_2O (10 mL) and saturated aqueous $NaHCO_3$ (60 mL), and extracted with EtOAc (3×50 mL). The combined organic layers were dried over $MgSO_4$, filtered and evaporated to give **32** (970 mg, 56%) as a white solid; mp: 120–121 °C; ^{1}H NMR (400 MHz, CD_3OD): δ = 4.61 (s, 2H, CH_2Br), 7.83 (t, J = 1.7 Hz, 1H, H-C(4)), 7.92 (t, J = 1.7 Hz, 1H, H-C(6)), 7.97 ppm (t, J = 1.7 Hz, 1H, H-C(2)); ^{13}C NMR (101 MHz, CD_3OD): δ = 31.40, 123.58, 126.51, 129.73, 136.39, 143.25, 147.45 ppm; IR (ATR): $\tilde{\nu}$ = 3342 (m), 3249 (m), 1566 (w), 1429 (w), 1317 (s), 1297 (m), 1230 (w), 1208 (m), 1157 (s), 1111 (w), 922 (m), 884 (m), 779 (m), 682 cm^{-1} (m); HR-ESI-MS (negative mode): m/z (%): 329.8457 (50, $[M-H]^-$ calcd for $C_7H_6{}^{81}Br_2NO_2S^-$: 329.8449), 327.8476 (100, $[M-H]^-$ calcd for $C_7H_6{}^{81}Br{}^{79}BrNO_2S^-$: 327.8471), 325.8498 (44, $[M-H]^-$ calcd for $C_7H_6{}^{79}Br_2NO_2S^-$: 325.8491).

3-[(3-Aminoisoquinolin-6-yl)methyl]-5-bromobenzenesulfonamide (36): A solution of isoquinoline **34** (212 mg, 0.50 mmol), bis(pinacolato)diboron (135 g, 0.53 mmol), and KOAc (119 mg, 1.50 mmol) in 1,4-dioxane (10 mL) was degassed for 10 min, treated with $[Pd(PPh_3)Cl_2]$ (37 mg, 0.05 mmol), and stirred for 4 h at 80 °C. After addition of Cs_2CO_3 (1.06 g, 1.50 mmol), degassed H_2O (0.5 mL), and compound **32** (265 mg, 0.60 mmol), stirring was continued for 2 h. The mixture was filtered over silica, eluting with EtOAc (50 mL). Chromatography (SiO_2, EtOAc/cyclohexane 1:2→1:1→2:1) afforded **36** (70 mg, 36%) as a yellow oil. R_f = 0.32 (SiO_2, EtOAc/cyclohexane 1:2); ^{1}H NMR (400 MHz, $CDCl_3$): δ = 1.45 (s, 18H, 2CMe_3), 4.19 (s, 2H, CH_2), 5.00 (br s, 2H, SO_2NH_2), 7.39 (d, J = 8.6 Hz, 1H, H-C(7′)), 7.53–7.59 (m, 2H, H-C(4′, 5′)), 7.60 (br s, 1H, H-C(4)), 7.72 (br s, 1H, H-C(2)), 7.91–7.95 (m, 2H, H-C(5, 8′)), 9.11 ppm (s, 1H, H-C(1′)); ^{13}C NMR (101 MHz, CD_3OD): δ = 27.97, 41.64, 83.22, 117.74, 123.30, 125.49, 126.23, 126.58, 127.73, 128.28, 128.77, 136.13, 137.68, 141.65, 143.46, 144.09, 147.47, 151.56, 151.83 ppm; IR (ATR): $\tilde{\nu}$ = 3329 (br w), 2980 (m), 1781 (m), 1738 (m), 1633 (m), 1566 (w), 1368 (m), 1339 (m), 1280 (m), 1249 (m), 1153 (s), 1104 (s), 948 (m), 912 (m), 729 cm^{-1} (s); HR-ESI-MS: m/z (%): 594.1094 (10, $[M+H]^+$ calcd for $C_{26}H_{31}{}^{81}BrN_3O_6S^+$: 594.1094), 592.1109 (10, $[M+H]^+$ calcd for $C_{26}H_{31}{}^{79}BrN_3O_6S^+$: 592.1111), 437.9942 (100, $[M-2C_4H_8-CO_2+H]^+$ calcd for $C_{17}H_{15}{}^{81}BrN_3O_4S^+$: 437.9946), 435.9962 (88, $[M-2C_4H_8-CO_2+H]^+$ calcd for $C_{17}H_{15}{}^{79}BrN_3O_4S^+$: 435.9967).

5-[(3-Aminoisoquinolin-6-yl)methyl]-4′-(trifluoromethyl)-[1,1′-biphenyl]-3-sulfonamide (20g): A solution of **34** (100 mg, 0.17 mmol), 4-(trifluoromethyl)phenylboronic acid (39 mg, 0.20 mmol), and Cs_2CO_3 (165 mg, 0.51 mmol) in 1,4-dioxane (5 mL) was degassed for 10 min, treated with $[PdCl_2(dppf)]\cdot CH_2Cl_2$ (14 mg, 0.02 mmol), and stirred for 50 min at 80 °C. The mixture was filtered over silica, eluting with EtOAc (50 mL) and evaporated. A solution of the residue in CH_2Cl_2 (4 mL) was cooled to 0 °C and treated with TFA (0.15 mL), stirred for 14 h, and evaporated. Chromatography (SiO_2, CH_2Cl_2/MeOH/NH_3 95:4:1) afforded **20g** (51 mg, 66%) as a white solid. R_f = 0.21 (SiO_2, CH_2Cl_2/MeOH/NH_3 95:4:1); mp: 223–224 °C; ^{1}H NMR (400 MHz, $(CD_3)_2SO$): δ = 4.20 (s, 2H, CH_2), 5.88 (br s, 2H, $ArNH_2$), 6.57 (s, 1H, H-C(4″)), 7.08 (dd, J = 7.4, 1.6 Hz, 1H, H-C(7″)), 7.40 (br s, 2H, SO_2NH_2), 7.45 (br s, 1H, H-C(5″)), 7.71 (d, J = 7.4 Hz, 1H, H-C(8″)), 7.76 (t, J = 1.7 Hz, 1H, H-C(2)), 7.88 (d, J = 8.4 Hz, 2H,H-C(2′, 6′), 7.93 (d, J = 8.4 Hz, 2H, H-C(3′, 5′)), 7.96 (t, J = 1.7 Hz, 1H, H-C(4)), 8.02 (t, J = 1.7 Hz, 1H, H-C(6)), 8.76 ppm (s, 1H, H-C(1″)); ^{13}C NMR (101 MHz, $(CD_3)_2SO$): δ = 41.07, 96.96, 121.29, 122.10, 123.17, 123.21, 124.21 (q, ^1J(C,F) = 271.9 Hz), 125.43, 126.04 (q, ^3J(C,F) = 3.7 Hz), 127.63, 128.11, 128.48 (q, ^2J(C,F) = 31.6 Hz), 130.76, 138.74, 139.45, 142.19, 142.68, 142.89, 145.20, 150.97, 156.64 ppm; ^{19}F NMR (282 MHz, $(CD_3)_2SO$): δ = −60.98 ppm; IR (ATR): $\tilde{\nu}$ = 3370 (w), 3312 (w), 1636 (m), 1496 (w), 1447 (w), 1347 (w), 1323 (s), 1148 (m), 1125 (m), 1110 (m), 1062 (w), 899 (w), 840 cm^{-1} (m); HR-ESI-MS: m/z (%): 458.1151 (100, $[M+H]^+$ calcd for $C_{23}H_{19}F_3N_3O_2S^+$: 458.1145).

Acknowledgements

We thank the ETH Research Council and the Hans Fischer Gesellschaft e.V. for their generous support of this research. We are grateful to Dr. Bruno Bernet (ETH) for proofreading the Experimental Section and to Anatol Schwab, Dr. Tristan Reekie, and Oliver Dumele for proofreading the entire manuscript. We are thankful to Michael Solar for recording the crystal structures.

Keywords: bis-sulfonamides · docking · inhibitors · isoprenoid biosynthesis · non-mevalonate pathway · *P. falciparum*

[1] W. Eisenreich, M. Schwarz, A. Cartayrade, D. Arigoni, M. H. Zenk, A. Bacher, *Chem. Biol.* **1998**, *5*, R221 – R233.
[2] M. Rohmer, *Nat. Prod. Rep.* **1999**, *16*, 565 – 574.
[3] A. R. Odom, W. C. Van Voorhis, *Mol. Biochem. Parasitol.* **2010**, *170*, 108 – 111.

[4] T. Haemers, J. Wiesner, S. Van Poecke, J. Goeman, D. Henschker, E. Beck, H. Jomaa, S. Van Calenbergh, *Bioorg. Med. Chem. Lett.* **2006**, *16*, 1888–1891.
[5] M. Rohmer, M. Seemann, S. Horbach, S. Bringer-Meyer, H. Sahm, *J. Am. Chem. Soc.* **1996**, *118*, 2564–2566.
[6] C. M. Crane, J. Kaiser, N. L. Ramsden, S. Lauw, F. Rohdich, W. Eisenreich, W. N. Hunter, A. Bacher, F. Diederich, *Angew. Chem. Int. Ed.* **2006**, *45*, 1069–1074; *Angew. Chem.* **2006**, *118*, 1082–1087.
[7] Z. Zhang, S. Jakkaraju, J. Blain, K. Gogol, L. Zhao, R. C. Hartley, C. A. Karlsson, B. L. Staker, T. E. Edwards, L. J. Stewart, P. J. Myler, M. Clare, D. W. Begley, J. R. Horn, T. J. Hagen, *Bioorg. Med. Chem. Lett.* **2013**, *23*, 6860–6863.
[8] J. Geist, S. Lauw, V. Illarionova, B. Illarionov, M. Fischer, T. Gräwert, F. Rohdich, W. Eisenreich, J. Kaiser, M. Groll, C. Scheurer, S. Wittlin, J. Alonso-Gómez, W. B. Schweizer, A. Bacher, F. Diederich, *ChemMedChem* **2010**, *5*, 1092–1101.
[9] F. Yüksel, A. G. Gürek, C. Lebrun, V. Ahsen, *New J. Chem.* **2005**, *29*, 726–732.
[10] V. Illarionova, J. Kaiser, E. Ostrozhenkova, A. Bacher, M. Fischer, W. Eisenreich, F. Rohdich, *J. Org. Chem.* **2006**, *71*, 8824–8834.
[11] F. Rohdich, W. Eisenreich, J. Wungsintaweekul, S. Hecht, C. A. Schuhr, A. Bacher, *Eur. J. Biochem.* **2001**, *268*, 3190–3197.
[12] R. E. Desjardins, C. J. Canfield, J. D. Haynes, J. D. Chulay, *Antimicrob. Agents Chemother.* **1979**, *16*, 710–718.
[13] A. J. Blacker, E. Clot, S. B. Duckett, O. Eisenstein, J. Grace, A. Nova, R. N. Perutz, D. J. Taylor, A. C. Whitwood, *Chem. Commun.* **2009**, 6801–6803.
[14] R. J. Alvarado, J. M. Rosenberg, A. Andreu, J. C. Bryan, W.-Z. Chen, T. Ren, K. Kavallieratos, *Inorg. Chem.* **2005**, *44*, 7951–7959.
[15] K. Brameld, B. Kuhn, D. C. Reuter, M. Stahl, *J. Chem. Inf. Model.* **2008**, *48*, 1–24.
[16] E. Persch, O. Dumele, F. Diederich, *Angew. Chem. Int. Ed.* **2015**, *54*, 3290–3327; *Angew. Chem.* **2015**, *127*, 3341–3382.
[17] F. Biedermann, W. M. Nau, H.-J. Schneider, *Angew. Chem. Int. Ed.* **2014**, *53*, 11158–11171; *Angew. Chem.* **2014**, *126*, 11338–11352.
[18] H.-J. Schneider, *Angew. Chem. Int. Ed.* **2009**, *48*, 3924–3977; *Angew. Chem.* **2009**, *121*, 3982–4036.
[19] D. Cubrilovic, W. Haap, K. Barylyuk, A. Ruf, M. Badertscher, M. Gubler, T. Tetaz, C. Joseph, J. Benz, R. Zenobi, *ACS Chem. Biol.* **2014**, *9*, 218–226.
[20] J. A. Loo, *Mass Spectrom. Rev.* **1997**, *16*, 1–23.
[21] J. L. P. Benesch, C. V. Robinson, *Nature* **2009**, *462*, 576–577.
[22] J. M. Daniel, S. D. Friess, S. Rajagopalan, S. Wendt, R. Zenobi, *Int. J. Mass Spectrom.* **2002**, *216*, 1–27.
[23] M. Peschke, U. H. Verkerk, P. Kebarle, *J. Am. Soc. Mass Spectrom.* **2004**, *15*, 1424–1434.
[24] E. N. Kitova, A. El-Hawiet, P. D. Schnier, J. S. Klassen, *J. Am. Soc. Mass Spectrom.* **2012**, *23*, 431–441.
[25] J. N. Weiss, *FASEB J.* **1997**, *11*, 835–841.
[26] Y.-C. Cheng, W. H. Prusoff, *Biochem. Pharmacol.* **1973**, *22*, 3099–3108.
[27] For a discussion of differences in K_i and K_d values, see: M. Neeb, M. Betz, A. Heine, L. J. Barandun, C. Hohn, F. Diederich, G. Klebe, *J. Med. Chem.* **2014**, *57*, 5566–5578.
[28] B. M. Calisto, J. Perez-Gil, M. Bergua, J. Querol-Audi, I. Fita, S. Imperial, *Protein Sci.* **2007**, *16*, 2082–2088.
[29] P. E. F. O'Rourke, J. Kalinowska-Tłuścik, P. K. Fyfe, A. Dawson, W. N. Hunter, *BMC Struct. Biol.* **2014**, *14*, 1.
[30] G. Jones, P. Willett, R. C. Glen, *J. Mol. Biol.* **1995**, *245*, 43–53.
[31] G. Jones, P. Willett, R. C. Glen, A. R. Leach, R. Taylor, *J. Mol. Biol.* **1997**, *267*, 727–748.
[32] O. Korb, T. Stützle, T. E. Exner, *J. Chem. Inf. Model.* **2009**, *49*, 84–96.
[33] P. R. Gerber, K. Müller, *J. Comput.-Aided Mol. Des.* **1995**, *9*, 251–268.
[34] I. L. Alberts, K. Nadassy, S. J. Wodak, *Protein Sci.* **1998**, *7*, 1700–1716.
[35] D. W. Begley, R. C. Hartley, D. R. Davies, T. E. Edwards, J. T. Leonard, J. Abendroth, C. A. Burris, J. Bhandari, P. J. Myler, B. L. Staker, L. J. Stewart, *J. Struct. Funct. Genomics* **2011**, *12*, 63–76.
[36] C. Baumgartner, C. Eberle, F. Diederich, S. Lauw, F. Rohdich, W. Eisenreich, A. Bacher, *Helv. Chim. Acta* **2007**, *90*, 1043–1068.
[37] C. T. Supuran, *Bioorg. Med. Chem. Lett.* **2010**, *20*, 3467–3474.
[38] E. Mochida, Y. Suzuki, K. Yamaguchi, H. Ohnishi (Mochida Pharmaceutical Co. Ltd.), Pat No. EP 0068408 A1, **1983**.
[39] L. Huang, S. Liu, E. A. Lunney, S. P. Planken (Pfizer Inc.), Int. PCT Pub. No. WO 2007125405 A3, **2007**.
[40] K. Utimoto, Y. Wakabayashi, T. Horiie, M. Inoue, Y. Shishiyama, M. Obayashi, H. Nozaki, *Tetrahedron* **1983**, *39*, 967–973.
[41] E. Anselmi, M. Abarbri, A. Duchêne, S. Langle-Lamandé, J. Thibonnet, *Synthesis* **2012**, *44*, 2023–2040.
[42] The PyMOL Molecular Graphics System, version 1.5.0.4, Schrödinger LLC.
[43] ACD/Percepta, version 2015, Advanced Chemistry Development Inc., Toronto, ON (Canada), **2015**.

Received: August 28, 2015
Published online on October 5, 2015